Proceedings of the 4th International Conference of Control, Dynamic Systems, and Robotics (CDSR'17)
Toronto, Canada – August 21 – 23, 2017
Paper No. 135
DOI: 10.11159/cdsr17.135

Revised Propeller Dynamics and Energy-Optimal Hovering in a Monospinner

Mojtaba Hedayatpour[1], Mehran Mehrandezh[1], Farrokh Janabi-Sharifi[2]
[1]University of Regina
3737 Wascana Pkwy, Regina, Canada
hedayatm@uregina.ca; mehran.mehrandezh@uregina.ca
[2]Ryerson University
350 Victoria St, Toronto, Canada
fsharifi@ryerson.ca

Abstract - This paper presents modelling, control and simulation results of an unmanned aerial vehicle (UAV) with only one fixed motor spinning a tilted propeller called "Monospinner". This class of rotary-wing UAVs is gaining some significant attention since they can lead to the design and development of control strategies for safe landing in case of one single or multiple rotor failure. Furthermore, the studies on monospinners can lead to the development of the most energy-efficient rotary wing UAVs with a potential to render themselves as high-endurance flying machines. In a monospinner, unlike most flying vehicles with rotary wings, hovering is defined as maintaining the altitude while rotating about an axis that is fixed with respect to the vehicle. Therefore, not all degrees of motion can be fully controlled. However, the remaining controllable states of the machine will be good enough to maintain a stable altitude, or even to track a trajectory. For this purpose, a linear time-invariant system is derived for controlling the attitude. It is shown that by controlling the attitude, the direction of that fixed axis of rotation (i.e., a precession axis) can be controlled by which the altitude of the vehicle can be kept at constant. A complete aerodynamic model of the propeller experiencing fast rotations about the precession axis is presented for the first time followed by analysing the effect a tilting rotor can have on the total power required to maintain a constant altitude. The proposed dynamic model and the design were evaluated via a nonlinear simulation system.

***Keywords*:** Unmanned flying vehicles, minimum power flight, propeller, tilting rotors, monospinner, stable flight despite rotor failure.

1. Introduction

Unmanned Aerial Vehicles (UAVs) have been one of the most popular research topics in recent years. A special type of these vehicles with four motors, known as quadcopters, has gained more attention among roboticists due to their mechanical simplicity. These flying vehicles have been used in a variety of applications such as: inspection of infrastructures, object delivery, precision agriculture and even sports [1]- [3].

One class of small-scale UAVs with rotary wing widely studied falls under the Quadcopters category. Although quadcopters with four actuators are fairly simple to design, but they don't offer a minimalistic design. For example, Samara-type vehicle is a flying machine, inspired form the way a maple seed flies in the air, that has only two actuators. Its attitude is controlled passively and its position can be controlled by an aerodynamic control surface [4]. The propulsive force is generated by adding a propeller to the system. An example of a Samara-type vehicle can be found in [5].

Flapping wing vehicles with one or two actuators are another example of under-actuated flying vehicles. Like Samara-type vehicles, the attitude is controller passively and the position can be controlled by the two actuators [6]. In position control for flapping wing vehicles with only one actuator, only altitude can be controlled [7].

In multicopters, it can be shown that by using less than four actuators, three translational and two rotational degrees of freedom can still be controlled. In [8], control of quadcopters in case of one, two and three rotor failures were presented. In case of three rotor failures, it can be said that one can achieve the simplest design for under-actuated flying vehicles while having control over position and two rotational degrees of freedom. In [9], a flying vehicle with a single rotor was presented for the first time.

In this paper, modelling and control of a flying vehicle with only one motor and one propeller is presented. Because of the unbalanced torque in the system (i.e., the gravitational force, thrust, and reaction forces don't intersect), the vehicle will go through a fast rotational motion about a fixed axis. This rotational motion affects the performance of the propeller which is fully investigated in this paper for the first time.

The relationship between the required motor power to maintain a hover when tilting the rotor about the x-axis of the body frame (see Fig. 1) and the tilting angle of the robot was calculated for the first time as well. The nonlinear equations of rotational motion are then linearized around the optimal-power hover solution and a controller is designed to maintain the attitude, hence controlling the position of the vehicle. Finally, the results were validated via simulations.

This paper is organized as follows: In section 2, mathematical modelling and control strategy are presented including the effects of the fast rotational motion on propeller performance and the effects of tilting the motor about x-axis of the body frame. Simulation results and optimal-power hover solution are presented in section 3. Finally, conclusions and future works are presented in section 4.

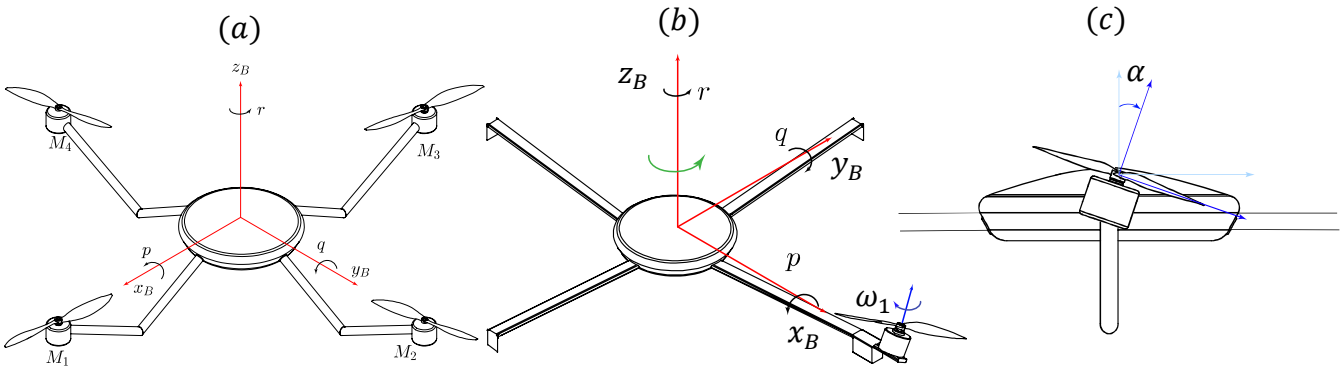

Fig. 1: a) A quadcopter with four motors, b) Unmanned flying vehicle with rotor (monospinner). Body frame is shown in red, b) The propeller angular velocity is negative and its reaction torque is positive. Because of the tilting angle of the motor, it also generates a positive moment about z-axis of the body frame as shown in green, c) The motor is tilted by alpha radians about x-axis.

2. Mathematical Modelling & Control

In this section mathematical modelling and control of the Monospinner are presented. Equations governing rotational motion are presented followed by equations of translational motion and a complete model for propeller's dynamics in presence of freestream velocity. Using nonlinear equations of motion, the equilibrium point is found for hovering. Nonlinear equations are then linearized around the equilibrium point. At the end, cascaded controller structure is used to control attitude and position of the vehicle.

2.1. Notation

Throughout this paper, straight boldface **R** is used for rotation matrices and vectors are shown in boldface italicized letters. Transformation from frame A to frame B is represented as ${}^{B}\mathbf{R}_{A}$. Boldface and non-boldface symbols are used to denote vectors and scalars respectively. The term ${}^{B}\omega_{B}$ denotes that ω is a property of B and is expressed in frame B. Top right superscript as in ω^{B} indicates that ω belongs to B. The vehicle angular velocity vector is shown as $\boldsymbol{\omega}^{B} = (p, q, r)^{T}$ where p, q and r are roll, pitch and yaw rates respectively. An overbar is used to indicate equilibrium values. Norm of a vector is shown by $|.|$.

2.2. Dynamic Model

Two coordinate frames are used for modelling. An inertial frame I that is attached to the earth and a body frame B that is attached to the centre of mass of the vehicle. The vehicle has a mass of m and the motor is located at distance l from the centre of mass of the vehicle. The motor is also tilted about x-axis of the body frame by α radians such that the propeller generates a thrust force $\boldsymbol{f}$ with components in y and z directions of the body frame. The position of the centre of mass of the vehicle in inertial frame is shown as $\boldsymbol{d}$ and earth gravitational acceleration is shown as $\boldsymbol{g}$. Using Newton's second law, the equations of translational motion can be written as follows:

$$m\ddot{\boldsymbol{d}} = {}^{I}\mathbf{R}_{B}\boldsymbol{f} + m\boldsymbol{g} \tag{1}$$

In (1), we assume that translational velocity of the centre of mass of the vehicle is low and thus, the drag due to this translational motion can be neglected. The geometry of the vehicle is assumed to be symmetric with a diagonal moment of inertia matrix as $\mathrm{I^B}=\mathrm{diag}(\mathrm{I_{xx}},\mathrm{I_{yy}},\mathrm{I_{zz}})$. The moment of inertia of the propeller is also represented by $I^p = \mathrm{diag}(\mathrm{I^p_{xx}}, \mathrm{I^p_{yy}}, \mathrm{I^p_{zz}})$ and is approximated by the moment of inertia of a disk which is also symmetric about propeller's axis of rotation.

The equation of rotational motion can be written as:

$$I^B\dot{\boldsymbol{\omega}}^B + I^p\dot{\boldsymbol{\omega}}^p + sk(\boldsymbol{\omega}^B)\left(I^B\boldsymbol{\omega}^B + I^p(\boldsymbol{\omega}^p + \boldsymbol{\omega}^B)\right) = \boldsymbol{\tau}_{tot} \tag{2}$$

In the left hand side of (2), the first two terms are the moments generated by angular acceleration of the body and the propeller. The third term represents cross-coupling effects of the angular momentum in the system. $sk(\boldsymbol{\omega}^B)$ is the skew symmetric matrix of body angular rates vector $\boldsymbol{\omega}^B$. Since $I^p \ll I^B$, the second term in (2) can be neglected. In the right hand side, $\boldsymbol{\tau}_{tot}$ is the summation of the moments due to propeller thrust force, reaction moment of the propeller as $\boldsymbol{\tau}_p^{reaction}$, aerodynamic drag in rotational motion as $\boldsymbol{\tau}_d$ and the moment due to unsymmetrical distribution of thrust between the advancing and retreating blades of the propeller as $\boldsymbol{\tau}^p$. Since yaw is the dominant rotational motion, $\boldsymbol{\tau}_d$ is considered only to oppose yaw motion and is assumed to be proportional to yaw rate with coefficient β as follows:

$$\boldsymbol{\tau}_d = (0,0,-\beta r)^T \tag{3}$$

Equations (1) and (3) can be combined and rewritten as follows:

$$\begin{gathered} m\begin{bmatrix}\ddot{d}_1\\ \ddot{d}_2\\ \ddot{d}_3\end{bmatrix} = {}^{I}\mathbf{R}_{B}\begin{bmatrix}0\\ fsin(\alpha)\\ fcos(\alpha)\end{bmatrix} + m\begin{bmatrix}0\\ 0\\ -9.81\end{bmatrix} \\ I_{xx}\dot{p} = -qr(I_{zz} - I_{xx}) - I^p_{zz}q\omega_1 \\ I_{yy}\dot{q} = -fcos(\alpha)l + pr(I_{zz} - I_{xx}) + I^p_{zz}p\omega_1 + \tau^p \\ I_{zz}\dot{r} = \tau_p^{reaction} + fsin(\alpha)l - \beta r \end{gathered} \tag{4}$$

Where ω_1 is the angular velocity of the propeller. $\tau_p^{reaction}$ is the reaction moment of the propeller. The reaction moment of the propeller is assumed to be proportional to thrust force and in the opposite direction of rotation of the propeller with a constant k_τ as follows:

$$\tau_p^{reaction} = -sign(\omega_1)k_\tau f \tag{5}$$

2.3. Propeller's Dynamics in Presence of Freestream Velocity

Freestream velocity, represented by V_∞, could have significant effects on performance of propellers. In the presence of none-zero freestream velocity, as the propeller is turning, the velocity of local air flow over the blades can be increased or decreased by V_∞ depending on the azimuth of the blades. As a result, the thrust force of the advancing blade would be different from that of the retreating blade which generates a moment. Our goal is to find the thrust force and moment of the propeller as a function of propeller and flow properties and freestream velocity. Blade element theory is used to calculate thrust force and moment of a blade element (small hashed area in Fig. 2 (b)) and by integrating them over all elements and azimuth angles, total thrust force and moment of the propeller can be calculated [10].

In Fig. 2 (b), a propeller with chord c and blade radius of R_b is turning counter-clockwise with angular velocity ω and there is a freestream velocity V_∞ (m/s) as shown with red arrows. The propeller azimuth ψ_p, is defined as the angle between the blade radius and the direction of freestream velocity. For a blade element of width dr_b and length c (the chord of the aerofoil) as shown in Fig. 2 (b), thrust force can be written as $df = \frac{1}{2}\rho c C_L v^2 dr_b$.

Where ρ is the air density, v is the resultant air flow velocity over the blade element at distance r_b from the propeller axis of rotation (that is the resultant of velocity due to the rotation of the propeller and freestream velocity) and C_L is the aerodynamic lift coefficient. It is also assumed that the blade chord is constant along the blade radius.

The freestream velocity affects the resultant air flow velocity over the blade element. For the advancing blade (when $0 \leq \psi_p \leq \pi$), the air flow velocity increases by V_∞ while it decreases by V_∞ for the retreating blade (when $\pi \leq \psi_p \leq 2\pi$). This inequality in air flow velocity over blade element generates a moment in the direction of freestream velocity V_∞ and affects total thrust force of the propeller. Thrust force for a blade element can be rewritten as follows:

$$df = \left(\frac{1}{2}\rho c C_L (r_b\omega + V_\infty \sin\psi_p)^2\right) dr_b \tag{6}$$

By integrating (6) over blade radius and azimuth angle and multiplying by 2 (assuming each propeller has two blades), we can calculate average thrust force of the propeller and likewise the produced moment as a function of propeller's angular velocity and freestream velocity as follows:

$$f = \frac{1}{2}\rho c C_L \left(\frac{2R_b^3}{3}\omega^2 + V_\infty^2 R\right) \qquad \tau^p = \frac{1}{3}\rho c C_L R_b^3 \omega V_\infty \tag{7}$$

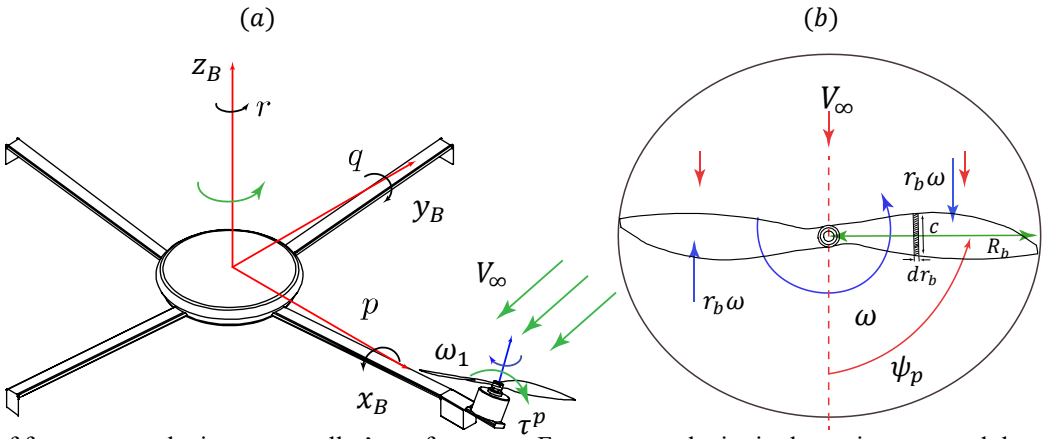

Fig. 2: a) Effects of freestream velocity on propeller's performance. Freestream velocity is shown in green and the propeller is turning clockwise as shown in blue. The asymmetrical lift distribution over the propeller, generates a positive pitch moment which could help to stabilize pitch motion. This moment is significant when the vehicle yaws very fast. b) Propeller turning counter-clockwise with angular velocity ω and freestream velocity is V_∞.

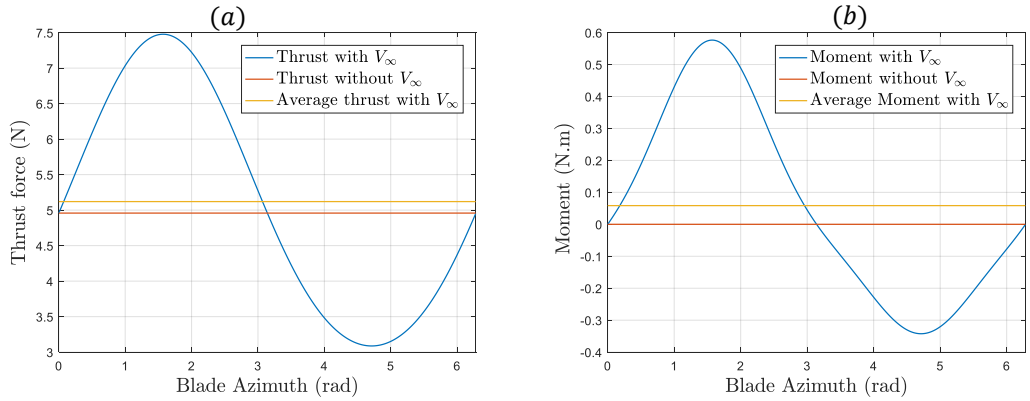

Fig. 3: Effects of having freestream velocity for a propeller with $c = 0.03\ m$, $C_L = 1.022$, $R_b = 0.08\ m$, $V_\infty = 10\ m/s$, $\rho = 1.225\ kg/m^3$ and $\omega = 870\ rad/s$. a) Thrust force of the propeller, b) Moment of the propeller due unsymmetrical lift.

When the propeller is turning and freestream velocity is zero, τ^p would be zero and thrust force would be equal to $f = \frac{1}{4}\rho c C_L \frac{2R_b^3}{3}\omega^2$. These effects for a propeller with known aerodynamic properties are presented in Fig. 2.

In order to see how thrust force and moment of the propeller change with azimuth angle, using (6) and (7), thrust force and moment of the propeller in one complete turn for $0 \leq \psi_p \leq 2\pi$ are calculated. Fig. 3, shows the results of this calculation for a propeller turning with angular velocity of $\omega = 870\, rad/s$ where there is a freestream velocity of $V_\infty = 10\, m/s$. Fig. 3 (a) and Fig. 3 (b), show variations of the thrust force and moment of the propeller as a function of azimuth angle respectively. The red color shows the calculated values without considering the effects of V_∞, the blue color shows calculated values with the effects of V_∞ and the yellow color shows the average values when considering the effects of V_∞. It can be seen that for $0 \leq \psi_p \leq \pi$, thrust force and moment are increased and for $\pi \leq \psi_p \leq 2$ they are decreased. The results show that the increase rate is more than decrease rate which is why the average values considering the effects of V_∞ are higher than the values without considering the effects of V_∞. In the above example, thrust force increases from 4.95 N to 5.12 N and the moment increases from 0 N.m to 0.06 N.m.

2.4. Control

Before designing a controller, one should define the equilibrium state of the system. In regular flying modes, equilibrium in flight is defined as a hovering state, where all velocities and accelerations of the vehicle are at zero. This is only possible if all forces and moments in the system are balanced. In a flying vehicle with only one rotor, forces and moments are not balanced and as a result, one cannot maintain zero velocities and accelerations in all directions. However, a new equilibrium state can be defined such that, for instance, all the angular velocities are constant and linear velocities are bounded, but periodic. In this equilibrium state, a fixed axis can be found about which the vehicle will rotate with constant angular velocity. By controlling the direction of this axis, the position of the vehicle can be controlled.

Let us denote this precession axis as $\boldsymbol{n}$ and present it in the body frame. The evolution of this axis in time can be given as:

$$\dot{\boldsymbol{n}} = -\boldsymbol{\omega}^B \times \boldsymbol{n} \tag{8}$$

At equilibrium, we want $\boldsymbol{n}$ to be constant, meaning that $\boldsymbol{n}$ should be parallel to $\boldsymbol{\omega}^B$. Therefore, by normalizing these vectors, the following condition must be met at the equilibrium state:

$$\dot{\boldsymbol{n}} = 0 \rightarrow |\bar{\boldsymbol{n}}| = \sigma|\bar{\boldsymbol{\omega}}^B| = 1 \tag{9}$$

At equilibrium, in order to maintain altitude, a component of the thrust force in the periodic motion should be equal to weight of the vehicle and in the opposite direction of the gravity, which adds the following constraint to the system:

$$\bar{f}\cos\alpha|\bar{n}_z| = m|\boldsymbol{g}| \tag{10}$$

Finally, by setting angular accelerations to zero, using (4) and (8)- (10), we will have eight unknowns as $\bar{p}, \bar{q}, \bar{r}, \bar{n}_x, \bar{n}_y, \bar{n}_z, \sigma, \bar{\omega}_1$ with eight algebraic equations. By solving this system of equations, we can find the equilibrium state of the vehicle. The tilting angle α, is a tuning parameter and we will discuss it in more details in the next section.

Now, nonlinear equations of rotational motion can be linearized about this equilibrium point and a controller for the resulting linear time-invariant system can be designed. In order to controller the position of the vehicle, controlling horizontal components of $\boldsymbol{n}$ is sufficient. For controlling altitude, the magnitude of the thrust force can be used. In this new equilibrium state, the vehicle is allowed to rotate about the fix axis $\boldsymbol{n}$. By defining and controlling a new state variable $\boldsymbol{\zeta} = (p, q, n_x, n_y)$, the two degrees of rotational motion (pitch and roll) can be controlled and as a result, the horizontal components of $\boldsymbol{n}$ can be controlled. Linearizing (4) and (8) about equilibrium state and choosing $\alpha = 0$, we can write the following first order differential equations for the deviation of $\boldsymbol{\zeta}$ from its equilibrium values $\bar{\boldsymbol{\zeta}}$:

$$\dot{\tilde{\boldsymbol{\zeta}}} = A\tilde{\boldsymbol{\zeta}} + B\boldsymbol{u} \quad , \quad u = \bar{f} - f \tag{11}$$

Similar to other flying vehicles, an outer control loop can be designed for position control which generates reference signal for the inner attitude controller. This can be simply done by defining $\tilde{\boldsymbol{d}}$ as the deviations of the position of the vehicle from the desired position. Finally, we can define the desired acceleration as a second order system with damping ratio ξ and natural frequency ω_n as follows:

$$\ddot{\boldsymbol{d}}_{des} = -2\xi\omega_n\dot{\tilde{\boldsymbol{d}}} - \omega_n^2\tilde{\boldsymbol{d}} \tag{12}$$

By calculating the desired acceleration and adding it to the gravity acceleration, total required acceleration is obtained. Now, using this total acceleration, the desired direction of $\boldsymbol{n}$ can be calculated as the reference of the attitude controller.

$$\boldsymbol{n_{des}} = \frac{m\ {}^{I}\mathbf{R}_B^T\left(\ddot{\boldsymbol{d}}_{des} - \boldsymbol{g}\right)}{f|\bar{n}_z|} \tag{13}$$

3. Simulation Results

In this section, simulation results for position control of a monospinner in four different scenarios are presented: 1) with $V_\infty=0$ and tilting angle $\alpha=0$; 3) with $V_\infty=0$ and non-zero tilting angle α; 3) with non-zero V_∞ and tilting angle $\alpha=0$; 4) with none-zero V_∞ and α. Power consumption in these simulations are compared. In monospinner, since the vehicle goes through a fast yaw motion, it can be said that the propeller's centre of mass goes through a rotation about the z-axis of the body frame and experiences an almost uniform freestream velocity which is approximately equal to $V_\infty = \bar{r}l$ (where l is the distance of the motor from the centre of mass of the vehicle). The direction of V_∞ is the negative direction of y-axis of the body frame. This freestream velocity can be expressed in the body frame as $V_\infty = (0, \bar{r}\bar{\omega}_1, 0)^T$.

From (7), as V_∞ increases, $\boldsymbol{\tau}^p$ increases which is in favor of balancing pitch moments. Also, since V_∞ is proportional to the vehicle's yaw rate at equilibrium. Therefore, higher yaw rate, which can be achieved by tilting the rotor, would be in favour of stabilizing the vehicle as well, meaning that we will need less control effort or less power to stabilize the system. Yaw rate, plays an important role and in fact this is the reason why we are tilting the rotor to increase yaw rate. We expect to see the highest power consumption in the first and second simulations and the lowest power consumption in the fourth simulation. At the end, the best value of α for optimal-power hover solution can be found.

It is also important to mention that the second and fourth simulations are more realistic since they capture all aerodynamic effects present in the system. The first and third simulations are only provided for comparison and showing that the effects of freestream velocity are not negligible especially in the case where the rotor is tilted.

A vehicle of mass $m = 0.5\,kg$, $I_{xx} = I_{yy} = 3.2 \times 10^{-3} kg.m^2$, $I_{zz} = 5.5 \times 10^{-3}\ kg.m^2$, $l = 0.17\,m$, $I_{zz}^p = 1.5 \times 10^{-5}\ kg.m^2$, $\beta = 2.75 \times 10^{-3}$, $k_\tau = 1.69 \times 10^{-2}$ is used in the simulations. The propeller has $c = 0.03\,m$, $C_L = 1.022$, $R_b = 0.08\,m$. Air density is $\rho = 1.225\,kg/m^3$. LQR controller for the LTI system in (11) with $Q = diag(1,1,100,100)$ and $R = 10$ as the weight matrices for attitude states and control input is designed. In position controller damping ratio $\xi = 0.5$ and natural frequency $\omega_n = 0.5$ are selected. To compare the simulation, power consumption of the motor is used. From [8], power consumption at equilibrium can be calculated as follows:

$$\bar{P} = \tau_p^{reaction}\bar{\omega}_1 = -sign(\bar{\omega}_1)k_\tau\bar{f}\bar{\omega}_1 \tag{14}$$

Table 1, shows equilibrium values for the simulations:

Table 1: Equilibrium values for the simulations.

Simulation condition	$\bar{p}\left(\frac{rad}{s}\right)$	$\bar{q}\left(\frac{rad}{s}\right)$	$\bar{r}\left(\frac{rad}{s}\right)$	$\bar{n}_x$	$\bar{n}_y$	$\bar{n}_z$	$\bar{\omega}_1\left(\frac{rad}{s}\right)$	$\bar{P}\ (W)$
V_∞=0 , α=0	14.6835	0	32.9938	0.4066	0	0.9136	-915.1880	83
$V_\infty = 5.6\ ,\ \alpha = 0$	15.1884	0	33.1648	0.4163	0	0.9091	-913.4880	83.3
$V_\infty = 0\ ,\ \alpha = 0.1$	6.5898	0	61.0706	0.1073	0	0.9942	-879.4980	73.6
$V_\infty = 10.4$, α=0.1	7.0300	0	61.1215	0.1142	0	0.9934	-865.3670	72.6

Comparing the power in the above simulations shows the significance of the effects of freestream velocity and tilting angle of the rotor in reducing power consumption of the motor. By selecting α as a tuning parameter we can find the best value of α and consequently the best value of V_∞ to find the minimum-power hover solution of the vehicle. The optimal-power solution is found when $\alpha = 0.25\ rad$, $V_\infty = \bar{r}l = 18.46\ m/s$ and the resulting power consumption is $\bar{P} = 72.1\ W$.

Simulation results for position control for flying from an initial position $d_0 = (0,0,10)$ to the desired position $d_{des} = (0,5,10)$ are presented in Fig. 4 and Fig. 5. In Fig. 4 (a), the thrust force of the propeller as function of time is presented. Fig. 4 (b), presents the angular velocity of the propeller as a function of time. Steady state results are shown in Fig. 5. According to (14), power consumption of the motor is proportional to the thrust force multiplied by the angular velocity of the propeller. In Fig. 5 (b), it can be seen that as α increases, the magnitude of angular velocity of the propeller decreases. From Fig. 5 (a), no specific correlation between α and the thrust force can be found. The angular velocity of the propeller at minimum-power hover solution is found to be $\bar{\omega}_{min} = 842.846\ rad/s$.

The oscillations shown in Fig. 5, are due to the periodic motion of the vehicle and the effects of the freestream velocity on the thrust force of the propeller as also presented in Fig. 3.

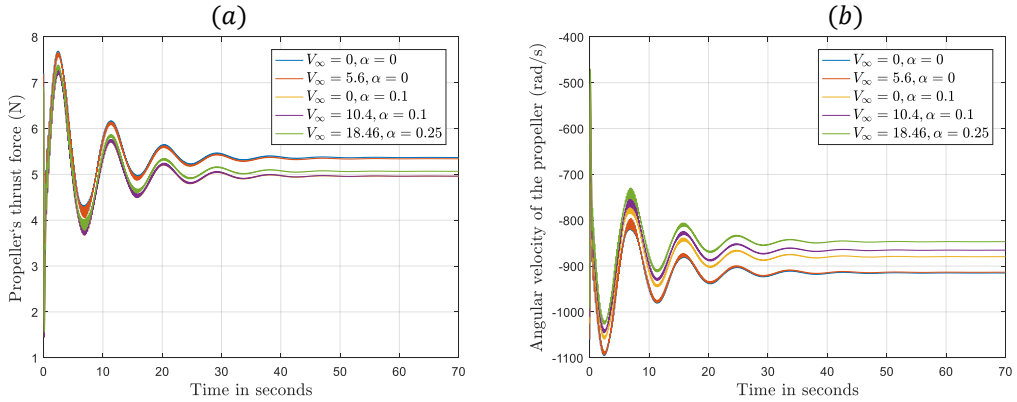

Fig. 4: Effects of freestream velocity and tilting angle of the rotor on: a) Thrust force of the propeller, b) Angular velocity of the propeller.

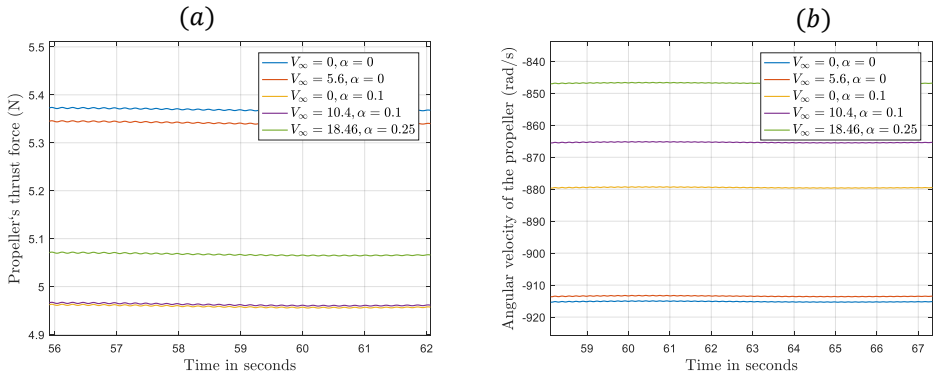

Fig. 5: Steady state values of: a) Thrust force of the propeller, b) Angular velocity of the propeller.

4. Conclusion

A flying vehicle with only one rotor is introduced in this paper. A complete mathematical model to capture all aerodynamic forces and moments in the system is presented and the equilibrium state of the system is found. The nonlinear equations of motion are then linearized around this equilibrium state. At equilibrium, the vehicle experiences a periodic motion and rotates about a fixed axis in space and can maintain its altitude by controlling the magnitude of thrust force generated by the propeller. By controlling the attitude of the vehicle, the direction of the fixed axis can be controlled. The average thrust force in the periodic motion is also in the direction of the fixed axis. Therefore, by controlling the direction of the fixed axis the position control can be achieved.

A complete model of the propeller operating in the presence of freestream velocity is presented and thrust and moment of the propeller (as a function of freestream velocity and angular velocity of the propeller) are calculated. Results show that effects of freestream velocity on propeller's performance are significant when there is a fast yaw motion in the system and the equilibrium point is far from that of when neglecting these effects.

The effects of tilting the motor about x-axis of the body frame is investigated next. Because of the cross-coupling effects of the angular momentum in the system, having a faster yaw motion helps to stabilize the vehicle. Simulation results for four different scenarios are presented and compared by power consumption of the motor. By choosing the tilting angle of the rotor as a tuning parameter and considering the effects of freestream velocity on propeller's performance (to make the model more realistic), optimal-power hover solution is found. At equilibrium and considering the effects of freestream velocity, the minimum power consumption in simulations is found to be $\bar{P}_{min} = 72.1\ W$ when the rotor is tilted by $\alpha = 0.25\ rad$, which is 13.5% lower than that of when $\alpha = 0$.

For future work, effects of tilting angle and freestream velocity on controller performance can be investigated. Sensitivity analysis for the proposed model could be another interesting topic for future work.

Acknowledgements

This research was supported by the Natural Sciences and Engineering Research Council of Canada (NSERC) and Micropilot Inc.

References

[1] J. Thomas, J. Polin, K. Sreenath, and V. Kumar, "Avian-inspired grasping for quadcopter micro UAVs," *Bioinspiration & Biomimetics*, vol. 9, pp. 25010-25019, 2014.

[2] P. Tokekar, J. Vander Hook, D. Mulla, and V. Isler. "Sensor Planning for a Symbiotic UAV and UGV System for Precision Agriculture," *IEEE Transactions on Robotics*, vol. 32, pp. 1498-1511, 2016.

[3] D. Mellinger, N. Michael, and V. Kumar, "Trajectory generation and control for precise aggressive maneuvers with quadcopters," in *Experimental Robotics*, vol. 31, no. 5, pp. 664-674, 2012.

[4] E. R. Ulrich, D. J. Pines, and J. S. Humbert, "From falling to flying: the path to powered flight of a robotic samara nano air vehicle," *Bioinspiration & biomimetics*, vol. 5, no. 4, pp. 045 009-045 025, 2010.

[5] S. Jameson, K. Fregene, M. Chang, N. Allen, H. Youngren, and J. Scroggins, "Lockheed martin's samarai nano air vehicle: Challenges, research, and realization," in *50th AIAA Aerospace Sciences Meeting, January*, pp. 1–21, 2012.

[6] K. Y. Ma, P. Chirarattananon, S. B. Fuller, and R. J. Wood, "Controlled flight of a biologically inspired, insect-scale robot," *Science*, vol. 340, no. 6132, pp. 603-607, 2013.

[7] Z. E. Teoh, S. B. Fuller, P. Chirarattananon, N. Prez-Arancibia, J. D. Greenberg, and R. J. Wood, "A hovering flapping-wing microrobot with altitude control and passive upright stability," in *IEEE/RSJ International Conference on Intelligent Robots and Systems (IROS)*. IEEE, pp. 3209–3216, 2012.

[8] M. W. Mueller and R. D'Andrea, "Stability and control of a quadrocopter despite the complete loss of one, two, or three propellers," *IEEE International Conference on Robotics and Automation (ICRA)*. IEEE, pp. 45–52, 2014.

[9] Weixuan Zhang, Mark W. Mueller, and Raffaello D'Andrea, "A controllable flying vehicle with a single moving part," *IEEE International Conference on Robotics and Automation (ICRA)*, 2016.

[10] J. D. Anderson, *Fundamentals of Aerodynamics*, 5*th* Ed. United States: McGraw Hill Higher Education, 2016, pp. 194-228.